

StarVector: Generating Scalable Vector Graphics Code from Images

Juan A. Rodriguez^{1,2,4} Shubham Agarwal^{1,2} Issam H. Laradji^{1,5} Pau Rodriguez^{6*}
David Vazquez¹ Christopher Pal^{1,2,3} Marco Pedersoli⁴

¹ServiceNow Research ²Mila - Quebec AI Institute ³Canada CIFAR AI Chair ⁴ÉTS, Montréal, Canada
⁵UBC, Vancouver, Canada ⁶Apple MLR, Barcelona, Spain * External collaboration

juan.rodriguez@mila.quebec

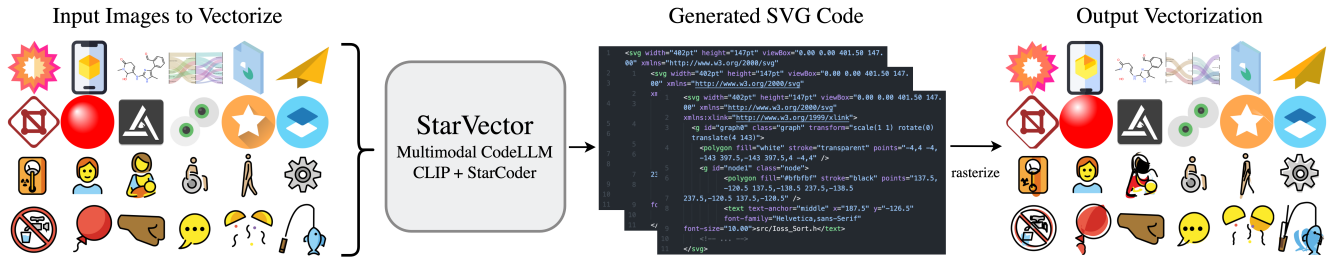


Figure 1. **Image-to-SVG generation task:** Given an input image, generate the corresponding SVG code. On the left, we show test examples of complex SVGs from SVG-Emoji and SVG-Stack datasets. StarVector encodes images and processes them in a multimodal language modeling fashion, to generate executable SVG code that resembles the input image. We show real generated code and rasterized images produced by our StarVector model, showing impressive capabilities at generating appealing SVG designs and using complex syntax.

Abstract

Scalable Vector Graphics (SVGs) have become integral in modern image rendering applications due to their infinite scalability in resolution, versatile usability, and editing capabilities. SVGs are particularly popular in the fields of web development and graphic design. Existing approaches for SVG modeling using deep learning often struggle with generating complex SVGs and are restricted to simpler ones that require extensive processing and simplification. This paper introduces StarVector, a multimodal SVG generation model that effectively integrates Code Generation Large Language Models (CodeLLMs) and vision models. Our approach utilizes a CLIP image encoder to extract visual representations from pixel-based images, which are then transformed into visual tokens via an adapter module. These visual tokens are pre-pended to the SVG token embeddings, and the sequence is modeled by the StarCoder model using next-token prediction, effectively learning to align the visual and code tokens. This enables StarVector to generate unrestricted SVGs that accurately represent pixel images. To evaluate StarVector’s performance, we present SVG-Bench, a comprehensive benchmark for evaluating SVG methods across multiple datasets and relevant metrics. Within this benchmark, we introduce novel

datasets including SVG-Stack, a large-scale dataset of real-world SVG examples, and use it to pre-train StarVector as a large foundation model for SVGs. Our results demonstrate significant enhancements in visual quality and complexity handling over current methods, marking a notable advancement in SVG generation technology. Code and models: <https://github.com/joanrod/star-vector>

1. Introduction

Vector Graphics represent an archetypal form of image representation, where visual compositions are constituted by primitive shapes such as vector paths, curves, or polygons, parametrized by mathematical equations [41]. This contrasts starkly with raster graphics, where images are represented as pixels on a grid. The primary advantage of vector graphics lies in their ability to maintain high precision and consistent visual quality across various resolutions, as they can be scaled arbitrarily without any loss of detail [34, 47].

In the realm of modern image rendering, Scalable Vector Graphics (SVGs) [54] have become a standard for encapsulating vector graphics in a code-based format. SVGs are the preferred choice for many artistic use cases like icon creation or typography. This format has gained prominence in applications demanding fast, efficient, and high-quality im-

age rendering. In web design, SVG contributes to enhanced rendering speeds and image compression owing to their inherently small file sizes. They also offer dynamic editability, allowing for straightforward modifications in color and size, which is crucial for accessibility and responsive design. For graphic design and scientific visualization, SVGs are prized for their visual quality, facilitating the creation of versatile designs and ensuring high-quality print outputs.

The SVG format utilizes Extensible Markup Language (XML) [26] syntax to define vector graphics, offering a rich palette for a broad range of graphical properties and effects. Central to SVG is the *vector path* (or simply path), comprised of points and control points connected by mathematically defined lines or curves, allowing detailed control over the shape and size of the graphics. SVGs can also incorporate a variety of other primitives, such as rectangles, ellipses, and text, along with styles and advanced capabilities.

Despite the eminent advantages of SVGs, existing deep learning-based generative solutions have limitations in producing high-quality, complex SVGs. Current approaches [12, 13, 61] typically model SVGs by learning a latent variable model over command paths. Such methods predominantly utilize simplified SVGs, limited to path commands and often restricted in complexity, with some focusing solely on elementary fonts or icons [79, 83]. Recent advancements involve using powerful image diffusion models [64] to generate raster images, which are then converted into SVG [34]. Nevertheless, it involves a costly iterative process of refinement and is also limited to paths. Despite these efforts, a gap remains in systems that can directly generate detailed and complex SVG code, leveraging the full range of SVG primitives necessary for intricate designs.

This paper studies the task of image-to-SVG generation (Figure 1), which has been traditionally approached as a form of image vectorization [42, 85], relying predominantly on image processing and curve fitting techniques [41, 78]. Our research diverges from these methods, posing the task as a code-generation problem building upon recent advancements in Large Language Models (LLMs) [9, 10, 74]. Thanks to the success in scaling up transformers [75], these models have shown outstanding downstream abilities in tasks like language understanding [16], summarization [71], or coding [40, 50, 65]. The emergent capabilities of LLMs in code creation are particularly relevant to our work, as shown by Bubeck et al. [10] in a study using GPT-4 [51] on generating SVG code.

In this work, we propose a novel paradigm, where a multimodal LLM learns SVG synthesis as an image-to-code generation task. In this new setting, we tackle the problem of image-to-SVG generation by learning a CLIP [57] image encoder coupled with an adapter model to project images into visual token embeddings (visual tokens) and use them to condition a StarCoder [40] model to generate an

SVG code associated with the input image. The StarVector architecture is shown in Figure 2. Addressing SVG generation with a code generation language model (CodeLLM) allows for preserving the richness and versatility of SVG primitives and syntax, as it can handle unaltered real-world SVGs and no need for simplification. Further, using the SVG code as a representation instead of a latent variable can bring enhanced editing capabilities. We propose the task of image-to-SVG as a pre-training task for building a foundation model [51, 74] for SVG generation.

Contributions. In summary, our contributions are the following: **i)** We introduce StarVector, a Large Multimodal Model for code generation, which leverages image and language modalities for generating executable SVG code from images. **ii)** We present SVG-Bench, a unified evaluation benchmark for SVG generation methods, which facilitates access to popular SVG datasets and metrics. Within this benchmark, we introduce two new datasets namely SVG-Emoji (composed of 10k complex emoji SVGs) and SVG-Stack (a large-scale dataset with over 2M real-world SVGs). **iii)** We evaluate StarVector and prior baselines on SVG-Bench which focuses on the image-to-SVG generation task. We showcase the ability of our model to generalize to complex SVGs and demonstrate the effectiveness of pre-training StarVector on the large-scale SVG-Stack dataset.

The paper is structured as follows: Section 2 presents previous methods related to our research on SVG generation while Section 3 explains the StarVector method in detail. We present SVG-Bench (with accompanying datasets and metrics) in Section 4, followed by experimental results in Section 5 and conclusions in Section 6.

2. Related Work

This section presents prior research relevant to our study, encompassing methods in vector graphics and SVG generation, developments in CodeLLMs, and advancements in multimodal models that integrate image and textual data.

SVG Generation Methods. Early efforts in vector graphics¹ predominantly utilized traditional image processing techniques for tasks like image vectorization [23, 42, 85], often involving segmentation and polynomial curve fitting [41, 78]. With the advent of deep learning, new approaches emerged. SVG-VAE [45], a class-conditional Variational Autoencoder (VAE) [35], predicts a latent style vector and generates SVGs using a LSTM decoder [30]. DeepSVG [13] proposes a hierarchical VAE architecture using transformers to represent SVG paths. Im2Vec [61] translates pixel images into latent representations, which

¹https://en.wikipedia.org/wiki/Comparison_of_raster-to-vector_conversion_software

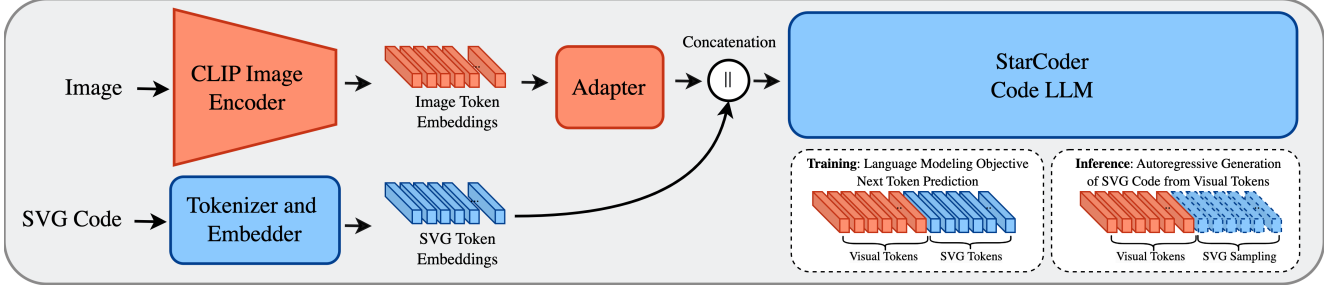


Figure 2. **StarVector architecture:** Images in the pixel space are encoded into a set of 2D embeddings using CLIP [56]. The Adapter applies a non-linear transformation to the image embeddings to align them with Code-LLM space, obtaining visual tokens. StarCoder uses the image embeddings as context to generate the SVG. During training the task is supervised by the next token prediction of the SVG tokens. During inference, the model uses the visual tokens from an input image to predict SVG code autoregressively.

can be decoded into paths via a recurrent neural network (RNN). However, latent-based methods are limited to path primitives, thus restricting their scope to a subset of SVGs. Because of this limitation, they tend to not generalize well and overfit on the complex-looking SVG datasets.

Recent trends in image generation using diffusion [29, 64] or autoregressive [25, 59, 86] models have also been explored in the SVG space. VectorFusion [34] leverages a strong text-to-image diffusion model to find the SVG via iterative optimization. CLIPasso [77] uses a CLIP distance loss to iteratively refine SVG from sketches. Both these solutions can be slow due to their iterative nature. Similar to ours, IconShop [83] trains a BERT [22] model for text-to-SVG conversion on icons, using path commands as tokens of the language model, while we use the SVG code.

This study addresses these challenges by proposing a new avenue in SVG modeling. We design a model capable of generating unrestricted SVG code, focusing on directly rendering vector graphics within the SVG code space, by-passing the constraints of previous methodologies.

Language Models for Code Generation. CodeLLMs, or large language models for code generation, have gained significant popularity in recent literature due to advances in natural language processing (NLP) and the transformer architectures [75], such as the GPT [9, 51, 55] and Llama [73, 74] families. Extensive availability of code datasets [8, 27, 32, 36], has allowed training powerful CodeLLMs that have changed the way software developers do their work [17]. Codex [14] learns to generate Python functions based on input docstrings and evaluates the correctness of the generated code samples automatically through unit tests. Codegen [50], studies multi-turn program synthesis under scaling laws, offering a family of models trained in several programming languages. StarCoder [40] presents a series of models with various sizes, trained on several coding languages using a fill-in-the-middle objective.

Despite SVG popularity, SVG language has been typi-

cally avoided in training large coding models [2, 40] (possibly for prioritizing more crowded coding communities). This research seeks to bridge this gap by fine-tuning a proficient CodeLLM specifically on SVG code. Furthermore, we integrate a vision module to facilitate the pre-training task of image-to-SVG conversion.

Multimodal Tasks and Models In recent years, there have been numerous works at the intersection of vision and language on topics like image captioning [37–39], visual question answering (VQA) [3], contrastive learning [15, 57] or text-to-image generation [25, 59, 60, 64]. For obtaining visual features some multimodal models [39, 48, 57] use Vision transformers (ViT) [24]. Convolutional-based image encoders like ConvNext [44] or VQGAN [25] have been also explored [25, 57, 64], that aim to preserve more detailed features from images. Some models like Flamingo [1], MAPL [48] or BLIP2 [39] use an intermediate mapping module to convert image features into fixed-size token embeddings. Similar to ours, Llava [43] obtains a set of visual tokens by projecting ViT features directly into the LLM embedding space.

While the majority of multimodal research has primarily been centered around a fusion of images and natural text [1, 39, 48, 57, 59], there has been relatively less attention to the process of translating images into code, except for few studies that convert web pages to HTML [20], image to Latex markup [21], GUI screenshot-to-code conversion [5, 7], and the generation of scientific vector graphics through Tikz [6]. This progress suggests that handling image generation as a coding task is an appealing solution. Our work explores different image-encoding techniques for the vision part and uses all available visual tokens to condition a StarCoder CodeLLM on images.

3. StarVector

This section describes StarVector, a multimodal code generation model that accepts images and generates compil-

able SVG code associated with it. We formulate the task of SVG generation as a sequence modeling problem, where sequences of tokens corresponding to the image and SVG domains are concatenated and modeled autoregressively. The proposed architecture is shown in Figure 2. StarVector integrates an Image Encoder i.e., CLIP, with a CodeLLM i.e., StarCoder through an Adapter layer. The Adapter converts image representations into visual tokens aligned with the SVG token embeddings used in the CodeLLM. After fine-tuning, image and text token embeddings share the same representation space, and the CodeLLM acquires SVG generation proficiency through next-token prediction, providing an effective solution for image-to-SVG conversion.

3.1. Image Encoder and Visual Tokens

The efficacy of our model relies heavily on the image encoder, which needs to preserve intricate details and semantic content in the original image because, unlike captioning, where the output is typically short, SVG generation requires generating much longer sequences of code to obtain results of higher complexity. The image encoder projects the input image into a set of 2D embeddings rich in fine-grained details. To choose the best encoder, we draw inspiration from the success of pre-trained encoder backbones in downstream computer vision tasks such as classification [57], retrieval, and generation [25], including both convolutional and transformer-based models. Formally, we experiment with CLIP ViT-L/14 [57], ConvNext [44] (both pre-trained on LAION-2B [66]), and VQGAN [25], which we pre-train on an image reconstruction task using raster images from SVG-Stack. As the output of the image encoder, we utilize all the available hidden representations in the last layers to bring the most rich features. We define the output of the encoder z_v as a flattened 2D grid of L_v embedding sequences. For CLIP we have $L_v = 257$ embeddings, including the CLS token. For VQGAN, we use the pre-quantization layers and flatten them to obtain $L_v = 196$ embeddings. For ConvNext, we flatten the last activation map to obtain $L_v = 49$ embeddings.

Adapter. The Adapter module performs a non-linear projection of the image embeddings into the LLM embedding space, producing a set of visual token embeddings (or visual tokens). This transformation matches the embedding dimensionality and aligns the image representations with the language model’s embedding space, effectively bridging the visual and SVG code modalities for the generation task. The Adapter is composed of a sequence of fully connected (FC) layers with Swish [58] activation function and Batch Normalization [33].

3.2. CodeLLM

The CodeLLM generates the complete SVG code conditioned on the visual tokens representing the image. We em-

ploy the StarCoder architecture by Li et al. [40] with pre-trained weights, which provide a general model for code completion tasks. StarCoder is a decoder-only architecture that uses Multi-Query Attention [68] for efficient sampling. To address the long sequence lengths and high memory demands, we use flash-attention [18], enabling fine-tuning StarCoder with a context length of 8,192 tokens, the only restriction of our models. This approach mitigates the quadratic complexity typically associated with neural attention in long sequences. The fine-tuning process updates all the model weights to overcome the distribution shift from the original pre-training task of general code generation to our specific task of image-to-SVG conversion. We emphasize that the pre-trained StarCoder is not trained to generate SVG code and thus needs to be fine-tuned end-to-end.

Training Process. During training, we first encode images x with the image encoder E as $E(x)$, which returns a hidden 2D features z_v of dimension $L_v \times D_v$, where L_v is the sequence length and D_v the embedding size. The adapter A projects z_v into the CodeLLM dimensionality as $A(z_v)$ resulting in visual tokens h_v of dimensionality $L_v \times D_l$, where D_l is the internal dimensionality of the CodeLLM. The ground truth SVG code is also tokenized and embedded into the CodeLLM space, as h_l , with the same dimensionality as the visual tokens h_v . During training, we concatenate visual and SVG token embeddings, and the sequence is modeled using standard language modeling training objective, i.e., next token prediction using SVG code as supervision. During inference, we only compute visual tokens from images and decode autoregressively from the CodeLLM with h_v as context.

4. SVGBench: Benchmark for SVG Validation

We propose SVGBench, a unified benchmark for assessing SVG synthesis models composed of tasks, datasets, and metrics. Here we evaluate the proposed StarVector and baselines on the task of image-to-SVG generation. This task has been the primary benchmark in previous works and assesses the model’s ability to generate SVG samples that resemble the input image in the pixel space. We aim to define a standardized evaluation setting for SVG generation, building upon popular practices in the recent literature [13, 45, 61]. In summary, we compile together the popular datasets and metrics used in prior works and propose new ones that define SVG-Bench.

4.1. Datasets

To encompass varying degrees of visual complexity across different colors, shapes, and text, we select datasets comprising examples of fonts, emojis, icons, and real-world examples e.g., the ones seen on websites. The datasets included in SVG-Bench are visually diverse and frequently

Dataset	Train	Val	Test	Test _{sim}	Source	Avg. Token Length	SVG Primitives
SVG-Fonts	1,831,857	91,593	4,821	3,745	Glypazzn [45]	2,121 ± 1,868	Vector path
SVG-Icons	80,442	6,256	2,449	1,277	DeepSVG [13]	2,449 ± 1,543	Vector path
SVG-Emoji	8,708	667	668	96	OpenMoji, NotoEmoji, TweMoji	2,551 ± 1805	All
SVG-Stack	2,169,710	108,456	5,709	1,585	TheStack [36]	1,822 ± 1,808	All

Table 1. **Datasets in SVG-Bench.** We show the number of samples per split, with an additional reduced test set composed of simplified SVGs. We facilitate the source where the dataset was acquired, and statistics about the length of the SVG code in tokens, considering the tokenizer trained by StarCoder [40]. Finally, we show the type of SVG primitives used in the datasets. SVG-Emoji and SVG-Stack are introduced in this paper. See Appendix 8 to see statistics and visualize samples from the datasets.

Model	Input	Output	Architecture	SVG Simplification	Seq Format	SVG commands	SVG primitives
Vtracer [78]	Image	SVG	Clustering + curve fitting	✓	Commands	M, L, C	Vector path
DeepSVG [13]	SVG	SVG	Transformer	✓	Commands	M, L, C	Vector path
Im2Vec [61]	Image	SVG	RNN	✓	Keypoints	M, L, C	Vector path
GPT-4 Vision [51]	Image	SVG	Multimodal LLM	×	SVG Code	All	All
StarVector (ours)	Image	SVG	Multimodal LLM	×	SVG code	All	All

Table 2. **Baseline comparison.** While prior works consider only 3 simple commands - M (Move), L (Line) and C (Curve), our model in principle can handle all type of complex SVG commands.

used by digital artists in real-life scenarios. We use SVG-Fonts introduced as Glypazzn [45] and SVG-Icons in DeepSVG [13]. In the absence of a standard benchmark, we create different splits for all the datasets, which we release to the community for further research. Following is a description of two datasets we propose for SVG generation.

SVG-Emoji We propose SVG-Emoji, a dataset of 10k image-SVG pairs created by collating multiple smaller emoji datasets from different sources into a unified dataset. Formally, we include examples from TweMoji², OpenMoji³ and NotoEmoji⁴, where we also provide information about their class and the corresponding caption.

SVG-Stack A key contribution of this work is SVG-Stack, a comprehensive, large-scale dataset of real-world SVGs, which we introduce as part of SVG-Bench. SVG-Stack is sourced from The Stack [36], a diverse dataset comprising code samples from various software languages, collated from public GitHub repositories⁵. Our selection builds upon the initial filtering and de-duplication processes conducted in [2, 36, 40]. We perform additional filtering to remove possible duplicates from other SVG datasets in the benchmark. We extracted SVG code from The Stack and rasterized it at 224x224 resolution to obtain ground truth images. This large amount of images, in conjunction with the SVG code, forms the foundation for pre-training StarVector, enabling it to learn the image-to-SVG conversion task effectively.

²<https://github.com/twitter/twemoji>

³<https://openmoji.org/>

⁴<https://github.com/googlefonts/noto-emoji>

⁵<https://huggingface.co/spaces/bigcode/in-the-stack>

Table 1 shows the dataset statistics defined in SVG-Bench. We create splits for train, validation, and test. We also create another test split using a pipeline of filtering and simplification to be consistent with the other baselines.

4.2. Evaluation Protocol

In evaluating SVG models, it is crucial to employ metrics that accurately measure the fidelity of the generated SVG with the original image, considering both vector and raster-pixel representations. Traditional pixel-based metrics may not be entirely adequate for SVG assessment, as the predominance of background colors can skew them. For instance, a simple SVG with a predominantly white background might misleadingly score well in these metrics. To address this, our evaluation framework also includes deep perceptual-based metrics and vector-space metrics, offering a more comprehensive and nuanced assessment of SVG conversion quality. We compute the following metrics:

- *Pixel-based metrics.* We employ Mean Squared Error (MSE) and Structural Similarity Index (SSIM) [80, 81]. MSE quantifies the average squared difference between the generated and the original images’ pixels, offering a straightforward measure of pixel-level accuracy. SSIM evaluates image quality based on the understanding of visual perception, measuring changes in structural information, luminance, and contrast.
- *Vector-based metrics.* We utilize Chamfer distance (CD), a metric adapted from point cloud literature [84]. This involves discretizing each SVG into a set of points by sampling paths at regular intervals. CD measures the average nearest-point distance between corresponding points in two SVGs, providing a quantitative measure of similarity. A smaller CD indicates that the two SVGs are more

similar, while a larger distance suggests they are more distinct. Having two SVGs s_1 and s_2 , defined with a set of points $p_1 \in s_1$ and $p_2 \in s_2$ in 2D, the CD is defined as,

$$c(s_1, s_2) = \frac{1}{|s_1|} \sum_{p_1 \in s_1} \min_{p_2 \in s_2} \|p_1 - p_2\|_2 + \frac{1}{|s_2|} \sum_{p_2 \in s_2} \min_{p_1 \in s_1} \|p_2 - p_1\|_2, \quad (1)$$

where $|s_i|$ is the cardinality of set s_i , and $\|\cdot\|_2^2$ is the squared Euclidean norm.

- *Perceptual-based Metrics.* We incorporate the Learned Perceptual Image Patch Similarity (LPIPS) [87] metric, which uses deep learning models trained on human perceptual judgments. This metric is particularly effective in capturing the nuances of human visual perception, providing a more subjective assessment of image quality beyond mere pixel-level comparisons.

4.3. Baselines

Here we describe the baselines used to compare StarVector’s performance in the task of image-to-SVG conversion. We consider previous deep learning-based methods and rule-based traditional methods. We evaluate the baselines with publicly available code in our proposed setup.

Im2Vec [61] uses an end-to-end VAE, trained using only image supervision to produce vector graphics. Input rasterized image is encoded to a ‘global’ latent vector, which is passed to an RNN to produce latent code for each path. The path decoder decodes these path codes into Bezier paths to generate the output SVG. We used the publicly available code⁶ to report the results.

DeepSVG [13] was introduced as a hierarchical path-based VAE encoder-decoder transformer architecture. Here input paths are encoded separately using a path encoder which are aggregated using a second encoder to produce a latent vector. The decoder uses this latent vector to output the path representations which provide actual draw commands and arguments. We used the open-source code⁷ to reproduce the results on different datasets. However, since the DeepSVG framework only allows simplified SVGs, we report results on the ‘simplified’ test set in Table 3.

VTracer⁸ [78] is a rule-based algorithm to convert images to SVGs. This 3-step pipeline algorithm relies on the hierarchical clustering of images which are traced into vectors. First, pixels are converted into paths, which are simplified into polygons. In the last step, polygons are smoothed and approximated with a Bezier curve fitter.

GPT-4-Vision (Preview) [52] was recently released by OpenAI as a vision-based multimodal model, with a limit of 100 API calls per day in the preview mode. We use GPT-4V by inserting an image and zero-shot prompting to generate SVG code. See Appendix 11 for more details.

⁶<https://github.com/preddy5/Im2Vec>

⁷<https://github.com/alexandre01/deepsvg>

⁸<https://github.com/visioncortex/vtracer>

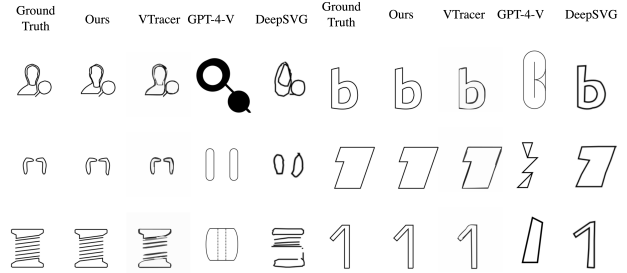


Figure 3. Results on simplified SVG-Icons and SVG-Fonts test.

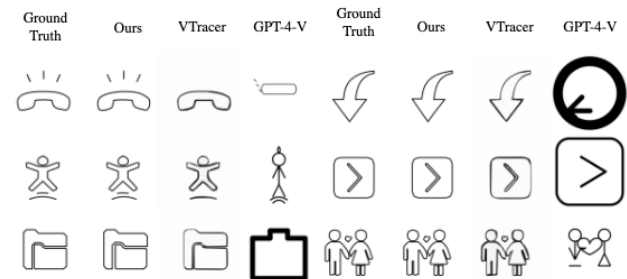


Figure 4. Results on SVG-Icons test set

5. Experiments and Results

This section presents the main experiments performed with the StarVector model on SVGBench. We report results on the simplified test as well as the full test set for the metrics defined in Section 4.2. We also ablate our model with different image encoders and data augmentation. Finally, we consider the effect of pre-training on SVG-Stack and fine-tuning on other datasets.

We use HuggingFace Transformers [82] and PyTorch [53] for the implementation. We reproduce baseline models from official repositories, respecting the proposed hyperparameters (see Appendix 11 for more detail). All experiments were done using 4 A100 80GB GPUs. We use a batch size of 2 with a gradient accumulation of 8 steps and a learning rate of 5×10^{-4} for training. Models trained on SVG-Stack with AdamW optimizer [46] require approximately 5 days of training.

Main results Results using the simplified test sets are shown in Table 3, created to accommodate the limitations of DeepSVG. Our model invariably outperforms Im2Vec and DeepSVG baselines on all the metrics. Our model also significantly outperforms the rule-based VTracer algorithm on Chamfer Distance (CD) while being comparable on the other metrics. Results on the complete test sets are depicted in Table 4. This setting considers substantially more examples with higher complexity, hence DeepSVG can not be evaluated here. StarVector improves over the Im2Vec base-

Method	SVG-Fonts _{sim}				SVG-Emojis _{sim}				SVG-Icons _{sim}				SVG-Stack _{sim}			
	MSE ↓	CD ↓	LPIPS ↓	SSIM ↑	MSE ↓	CD ↓	LPIPS ↓	SSIM ↑	MSE ↓	CD ↓	LPIPS ↓	SSIM ↑	MSE ↓	CD ↓	LPIPS ↓	SSIM ↑
VTracer [78]	0.014	5.631	<u>0.044</u>	0.946	0.018	<u>4.494</u>	0.064	0.911	0.009	3.885	<u>0.052</u>	0.952	0.016	4.983	0.061	0.918
DeepSVG [13]	0.046	<u>3.747</u>	0.163	0.823	0.069	5.486	0.278	0.748	0.04	<u>2.492</u>	0.153	0.851	0.066	<u>4.804</u>	0.235	0.736
Im2Vec [61]	0.031	133.977	0.187	0.871	0.042	26.457	0.258	0.826	0.029	146.616	0.178	0.885	0.043	138.031	0.258	0.813
GPT-4 Vision (100 examples)	0.091	65.103	0.248	0.755	0.099	52.206	0.268	0.701	0.128	50.649	0.271	0.709	0.131	55.455	0.28	0.668
StarVector (ours)	<u>0.019</u>	1.435	0.043	<u>0.93</u>	<u>0.038</u>	1.005	<u>0.073</u>	<u>0.859</u>	<u>0.018</u>	0.665	0.036	<u>0.931</u>	<u>0.038</u>	2.208	<u>0.098</u>	<u>0.858</u>

Table 3. **Results on simplified (sim) datasets** for the task of image-to-SVG conversion for different methods across SVGBench. Bold cells display the best model, and underlined cells show the second place (across all tables).

Method	SVG-Fonts				SVG-Emojis				SVG-Icons				SVG-Stack			
	MSE ↓	CD ↓	LPIPS ↓	SSIM ↑	MSE ↓	CD ↓	LPIPS ↓	SSIM ↑	MSE ↓	CD ↓	LPIPS ↓	SSIM ↑	MSE ↓	CD ↓	LPIPS ↓	SSIM ↑
VTracer [78]	0.007	4.105	<u>0.029</u>	<u>0.903</u>	0.007	<u>8.261</u>	0.064	0.913	0.014	<u>3.335</u>	<u>0.068</u>	0.927	0.007	<u>6.318</u>	0.057	0.891
Im2Vec [61]	0.133	144.413	0.208	0.802	0.124	39.135	0.528	0.658	0.052	145.497	0.221	0.831	0.179	141.573	0.357	0.688
GPT-4 Vision (100 examples)	0.194	27.909	0.268	0.689	0.162	21.134	0.404	0.612	0.135	49.249	0.299	0.666	0.192	16.981	0.37	0.604
StarVector (ours)	<u>0.008</u>	2.098	0.013	0.976	<u>0.051</u>	2.194	<u>0.202</u>	<u>0.778</u>	<u>0.022</u>	0.483	0.043	<u>0.923</u>	<u>0.072</u>	6.153	<u>0.153</u>	<u>0.785</u>

Table 4. **Results on complete datasets** for the task of image-to-SVG conversion. Metrics are computed on the full test sets of SVG-Bench. DeepSVG is not included as it does not support complex SVG images.

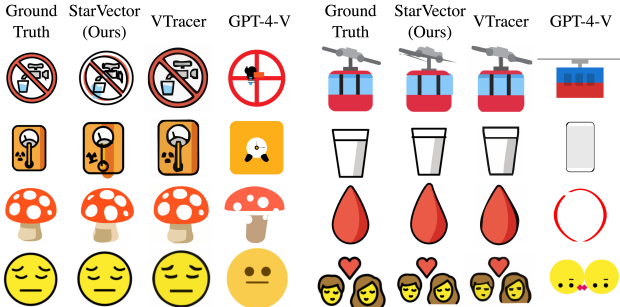


Figure 5. Results on SVG-Emoji test set

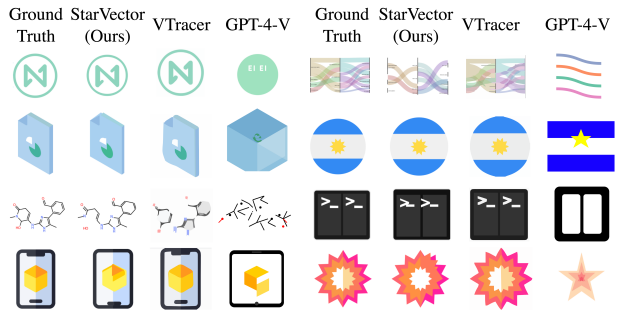


Figure 6. Results on SVG-Stack test set

line by a huge margin on all the metrics. Im2Vec performs very poorly on the CD metric for both the simplified as well as full test sets. StarVector outperforms VTracer on CD while being comparable in other metrics, signifying that our proposed approach learns to better mimic the ground truth SVG. We note that VTracer does not reason about the SVG generation as it is purely copying it. This limits VTracer for its use in other tasks such as text-to-SVG.

Notably, the MSE metric can sometimes yield misleading results. This is particularly evident in the performance of Im2Vec on the simplified datasets shown in Table 3 and SVG-Icons from Table 4, where it demonstrates seemingly good reconstruction. The reason lies in the simplified SVGs, which contain a significantly reduced number of pixels for representing the graphics, leading to a predominantly white background in the images. For the other datasets containing more pixels to represent the graphics, MSE for Im2Vec is more affected. In contrast, vector-based metrics like CD provides a more appropriate measure for assessing similarity. We also observe overfitting problems on DeepSVG and Im2Vec methods when training them on our setup. DeepSVG struggles to learn from SVG-Emoji due to limited data, while Im2Vec consistently overfits. We hypothesize that since Im2Vec is trained using only image supervision, it fails to generalize to complex SVGs.

Qualitative Evaluation We present the SVG images generated by different methods in Figure 3, for the simplified SVGs, and in Figures 5 and 6 for the complex SVG-Emoji and SVG-Stack datasets. StarVector generates appealing SVG conversions, with a comparable performance to VTracer. GPT-4 relies exclusively on semantic abilities to create the SVG, thus, losing fidelity at the pixel level, while our model preserves both semantic as well as fine-grained visual information. We also provide lemon-picked failure cases of our model in the Appendix.

Pre-training on SVG-Stack. Pre-training on the SVG-Stack is highly beneficial for the downstream datasets with small data. Table 5 shows the uplift on all the metrics for different datasets. Qualitatively, we can also see that pre-training helps the model to identify the nuanced details from

Visual encoder	SVG-Fonts				SVG-Emojis				SVG-Icons				SVG-Stack			
	MSE ↓	CD ↓	LPIPS ↓	SSIM ↑	MSE ↓	CD ↓	LPIPS ↓	SSIM ↑	MSE ↓	CD ↓	LPIPS ↓	SSIM ↑	MSE ↓	CD ↓	LPIPS ↓	SSIM ↑
CLIP	0.021	2.344	0.026	0.955	0.051	2.194	0.202	0.778	0.008	2.098	0.013	0.976	0.093	9.867	0.196	0.753
VQGAN	0.072	3.266	0.092	0.854	0.099	6.889	0.345	0.688	0.055	1.661	0.117	0.823	0.158	14.254	0.315	0.661
ConvNext	0.073	3.054	0.085	0.854	0.088	3.445	0.311	0.708	0.055	1.622	0.116	0.827	0.146	13.791	0.288	0.676

Table 5. **Ablation study** with different image encoders while keeping the rest of the architecture the same. CLIP as the backbone vision model performs the best in similar parameter settings.

Method	SVG-Emojis				SVG-Icons			
	MSE ↓	CD ↓	LPIPS ↓	SSIM ↑	MSE ↓	CD ↓	LPIPS ↓	SSIM ↑
StarVector (vanilla)	0.108	5.318	0.355	0.683	0.047	1.704	0.104	0.845
+ Data Augmentation	<u>0.097</u>	<u>3.796</u>	<u>0.329</u>	<u>0.706</u>	<u>0.029</u>	<u>0.707</u>	<u>0.057</u>	<u>0.905</u>
+ SVG-Stack Pre-train	0.061	2.047	0.225	0.748	0.031	0.712	0.057	0.894

Table 6. **Results on SVG data augmentation.** Smaller datasets prone to overfitting are evaluated in this experiment. “+” indicates that previous rows are also included.

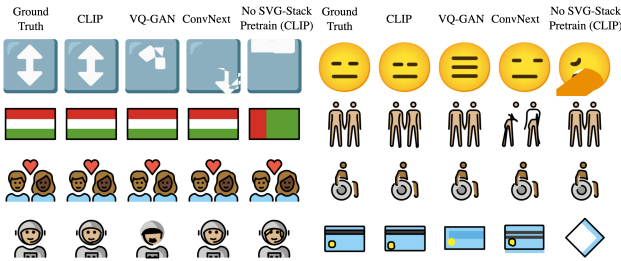


Figure 7. Ablation on SVG-emoji using different Visual encoders.

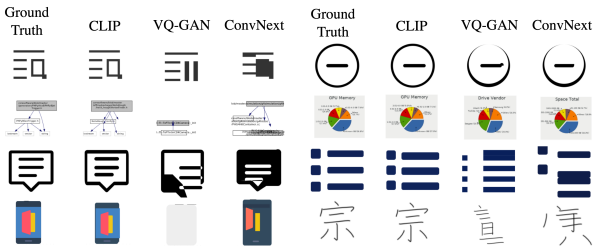


Figure 8. Ablation on SVG-Stack using different Visual encoders

the images. For the case of SVG-Emoji, pre-training is a strong requirement, as it overfits without it due to limited data. As shown in Figure 7, the model relies on colors and shapes to generate the SVG.

Data Augmentation We introduce several data augmentation operations on SVGs, that aim to perform small modifications to the SVG code and rasterize it to get a new sample while training. We include rotation, color noise, and curve noise (See Appendix 9 for more detail). We evaluate this setting on datasets that include fewer samples, namely SVG-Emoji and SVG-Icons, as the other two datasets are large enough to not overfit. Results are shown in Table 6.

Both datasets display improvements using these augmentations. We see a strong uplift for SVG-Emoji which has limited training data.

Ablation studies on Image Encoders We ablated with different visual encoders such as VQGAN [25] and ConvNext [44], however, we found CLIP consistently outperformed on all the metrics for different datasets (See Table 5). Figures 7 and 8, show qualitatively how VQGAN and ConvNext tend to lose local details during the generation while maintaining the relevant semantics.

6. Conclusions

We present StarVector, a novel multimodal CodeLLM that auto-regressively generates compilable SVG code from pixel images. Our model encodes images using a pre-trained CLIP encoder and generates vector graphics using a pre-trained StarCoder, which we fine-tune in an end-to-end fashion. Empirically, our model outperforms previous baselines for the image-to-SVG conversion task. We also present a standardized benchmark, SVG-Bench with two new datasets SVG-Stack and SVG-Emoji for further research on real-world SVG modeling.

Broader impact. With our current work, we aim to standardize and provide a reproducible benchmark consisting of a collection of SVG datasets and evaluation metrics. We believe our work will pave the way for future vector graphic generation models assisting digital artists.

Limitations and future work. While this work is limited to image-to-SVG generation, we consider our proposed approach and framework a first step towards building next-generation multimodal systems to create and edit SVG for logotype design, scientific diagram, and figure creation [62, 63]. Another limitation is the context length of 8k tokens on the generated SVGs, which we aim to overcome in future work using the recent success of CodeLLMs like CodeLlama [65].

Acknowledgments. We thank Arjun Ashok, Hector Laria, and Georges Bélanger for their valuable feedback and suggestions. We thank Raymond Li and Joel Lamy-Poirier for their assistance with StarCoder training.

References

- [1] Jean-Baptiste Alayrac, Jeff Donahue, Pauline Luc, Antoine Miech, Iain Barr, Yana Hasson, Karel Lenc, Arthur Mensch, Katherine Millican, Malcolm Reynolds, et al. Flamingo: a visual language model for few-shot learning. *Advances in Neural Information Processing Systems*, 35:23716–23736, 2022. [3](#)
- [2] Loubna Ben Allal, Raymond Li, Denis Kocetkov, Chenghao Mou, Christopher Akiki, Carlos Munoz Ferrandis, Niklas Muennighoff, Mayank Mishra, Alex Gu, Manan Dey, et al. Santacoder: don’t reach for the stars! *arXiv preprint arXiv:2301.03988*, 2023. [3](#), [5](#)
- [3] Stanislaw Antol, Aishwarya Agrawal, Jiasen Lu, Margaret Mitchell, Dhruv Batra, C Lawrence Zitnick, and Devi Parikh. Vqa: Visual question answering. In *Proceedings of the IEEE international conference on computer vision*, pages 2425–2433, 2015. [3](#)
- [4] Jimmy Lei Ba, Jamie Ryan Kiros, and Geoffrey E Hinton. Layer normalization. *arXiv preprint arXiv:1607.06450*, 2016. [1](#)
- [5] Daniel Baulé, Christiane Gresse von Wangenheim, Aldo von Wangenheim, Jean CR Hauck, and Edson C Vargas Júnior. Automatic code generation from sketches of mobile applications in end-user development using deep learning. *arXiv preprint arXiv:2103.05704*, 2021. [3](#)
- [6] Jonas Belouadi, Anne Lauscher, and Steffen Eger. Automatizk: Text-guided synthesis of scientific vector graphics with tikz. *arXiv preprint arXiv:2310.00367*, 2023. [3](#), [4](#)
- [7] Tony Beltramelli. pix2code: Generating code from a graphical user interface screenshot. In *Proceedings of the ACM SIGCHI Symposium on Engineering Interactive Computing Systems*, pages 1–6, 2018. [3](#)
- [8] Ekaba Bisong and Ekaba Bisong. Google bigquery. *Building Machine Learning and Deep Learning Models on Google Cloud Platform: A Comprehensive Guide for Beginners*, pages 485–517, 2019. [3](#)
- [9] Tom Brown, Benjamin Mann, Nick Ryder, Melanie Subbiah, Jared D Kaplan, Prafulla Dhariwal, Arvind Neelakantan, Pranav Shyam, Girish Sastry, Amanda Askell, et al. Language models are few-shot learners. *Advances in neural information processing systems*, 33:1877–1901, 2020. [2](#), [3](#)
- [10] Sébastien Bubeck, Varun Chandrasekaran, Ronen Eldan, Johannes Gehrke, Eric Horvitz, Ece Kamar, Peter Lee, Yin Tat Lee, Yuanzhi Li, Scott Lundberg, et al. Sparks of artificial general intelligence: Early experiments with gpt-4. *arXiv preprint arXiv:2303.12712*, 2023. [2](#), [3](#)
- [11] Mu Cai, Zeyi Huang, Yuheng Li, Haohan Wang, and Yong Jae Lee. Leveraging large language models for scalable vector graphics-driven image understanding. *arXiv preprint arXiv:2306.06094*, 2023. [1](#)
- [12] Defu Cao, Zhaowen Wang, Jose Echevarria, and Yan Liu. Svgformer: Representation learning for continuous vector graphics using transformers. In *Proceedings of the IEEE/CVF Conference on Computer Vision and Pattern Recognition*, pages 10093–10102, 2023. [2](#)
- [13] Alexandre Carlier, Martin Danelljan, Alexandre Alahi, and Radu Timofte. Deepsvg: A hierarchical generative network for vector graphics animation. *Advances in Neural Information Processing Systems*, 33:16351–16361, 2020. [2](#), [4](#), [5](#), [6](#), [7](#), [3](#)
- [14] Mark Chen, Jerry Tworek, Heewoo Jun, Qiming Yuan, Henrique Ponde de Oliveira Pinto, Jared Kaplan, Harri Edwards, Yuri Burda, Nicholas Joseph, Greg Brockman, et al. Evaluating large language models trained on code. *arXiv preprint arXiv:2107.03374*, 2021. [3](#)
- [15] Mehdi Cherti, Romain Beaumont, Ross Wightman, Mitchell Wortsman, Gabriel Ilharco, Cade Gordon, Christoph Schuhmann, Ludwig Schmidt, and Jenia Jitsev. Reproducible scaling laws for contrastive language-image learning. In *Proceedings of the IEEE/CVF Conference on Computer Vision and Pattern Recognition*, pages 2818–2829, 2023. [3](#)
- [16] Aakanksha Chowdhery, Sharan Narang, Jacob Devlin, Maarten Bosma, Gaurav Mishra, Adam Roberts, Paul Barham, Hyung Won Chung, Charles Sutton, Sebastian Gehrmann, et al. Palm: Scaling language modeling with pathways. *arXiv preprint arXiv:2204.02311*, 2022. [2](#)
- [17] Arghavan Moradi Dakhel, Vahid Majdinasab, Amin Nikanjam, Foutse Khomh, Michel C Desmarais, and Zhen Ming Jack Jiang. Github copilot ai pair programmer: Asset or liability? *Journal of Systems and Software*, 203:111734, 2023. [3](#)
- [18] Tri Dao, Dan Fu, Stefano Ermon, Atri Rudra, and Christopher Ré. Flashattention: Fast and memory-efficient exact attention with io-awareness. *Advances in Neural Information Processing Systems*, 35:16344–16359, 2022. [4](#), [3](#)
- [19] Jia Deng, Wei Dong, Richard Socher, Li-Jia Li, Kai Li, and Li Fei-Fei. Imagenet: A large-scale hierarchical image database. In *2009 IEEE conference on computer vision and pattern recognition*, pages 248–255. Ieee, 2009. [1](#)
- [20] Yuntian Deng, Anssi Kanervisto, and Alexander M Rush. What you get is what you see: A visual markup decompiler. *arXiv preprint arXiv:1609.04938*, 10:32–37, 2016. [3](#)
- [21] Yuntian Deng, Anssi Kanervisto, Jeffrey Ling, and Alexander M Rush. Image-to-markup generation with coarse-to-fine attention. In *International Conference on Machine Learning*, pages 980–989. PMLR, 2017. [3](#)
- [22] Jacob Devlin, Ming-Wei Chang, Kenton Lee, and Kristina Toutanova. Bert: Pre-training of deep bidirectional transformers for language understanding. *arXiv preprint arXiv:1810.04805*, 2018. [3](#)
- [23] James Richard Diebel. *Bayesian Image Vectorization: the probabilistic inversion of vector image rasterization*. Stanford University, 2008. [2](#)
- [24] Alexey Dosovitskiy, Lucas Beyer, Alexander Kolesnikov, Dirk Weissenborn, Xiaohua Zhai, Thomas Unterthiner, Mostafa Dehghani, Matthias Minderer, Georg Heigold, Sylvain Gelly, et al. An image is worth 16x16 words: Transformers for image recognition at scale. *arXiv preprint arXiv:2010.11929*, 2020. [3](#), [1](#)
- [25] Patrick Esser, Robin Rombach, and Bjorn Ommer. Taming transformers for high-resolution image synthesis. In *Proceedings of the IEEE/CVF conference on computer vision and pattern recognition*, pages 12873–12883, 2021. [3](#), [4](#), [8](#), [1](#)

- [26] Jon Ferraiolo, Fujisawa Jun, and Dean Jackson. *Scalable vector graphics (SVG) 1.0 specification*. iuniverse Bloomington, 2000. 2
- [27] Leo Gao, Stella Biderman, Sid Black, Laurence Golding, Travis Hoppe, Charles Foster, Jason Phang, Horace He, Anish Thite, Noa Nabeshima, et al. The pile: An 800gb dataset of diverse text for language modeling. *arXiv preprint arXiv:2101.00027*, 2020. 3
- [28] Xavier Glorot and Yoshua Bengio. Understanding the difficulty of training deep feedforward neural networks. In *Proceedings of the thirteenth international conference on artificial intelligence and statistics*, pages 249–256. JMLR Workshop and Conference Proceedings, 2010. 1
- [29] Jonathan Ho, Ajay Jain, and Pieter Abbeel. Denoising diffusion probabilistic models. *Advances in neural information processing systems*, 33:6840–6851, 2020. 3
- [30] Sepp Hochreiter and Jürgen Schmidhuber. Long short-term memory. *Neural computation*, 9(8):1735–1780, 1997. 2
- [31] Ari Holtzman, Jan Buys, Li Du, Maxwell Forbes, and Yejin Choi. The curious case of neural text degeneration. *arXiv preprint arXiv:1904.09751*, 2019. 3, 4
- [32] Hamel Husain, Ho-Hsiang Wu, Tiferet Gazit, Miltiadis Alamanis, and Marc Brockschmidt. Codesearchnet challenge: Evaluating the state of semantic code search. *arXiv preprint arXiv:1909.09436*, 2019. 3
- [33] Sergey Ioffe and Christian Szegedy. Batch normalization: Accelerating deep network training by reducing internal covariate shift. In *International conference on machine learning*, pages 448–456. pmlr, 2015. 4
- [34] Ajay Jain, Amber Xie, and Pieter Abbeel. Vectorfusion: Text-to-svg by abstracting pixel-based diffusion models. In *Proceedings of the IEEE/CVF Conference on Computer Vision and Pattern Recognition*, pages 1911–1920, 2023. 1, 2, 3
- [35] Diederik P Kingma and Max Welling. Auto-encoding variational bayes. *arXiv preprint arXiv:1312.6114*, 2013. 2
- [36] Denis Kocetkov, Raymond Li, Loubna Ben Allal, Jia Li, Chenghao Mou, Carlos Muñoz Ferrandis, Yacine Jernite, Margaret Mitchell, Sean Hughes, Thomas Wolf, et al. The stack: 3 tb of permissively licensed source code. *arXiv preprint arXiv:2211.15533*, 2022. 3, 5
- [37] Chenliang Li, Haiyang Xu, Junfeng Tian, Wei Wang, Ming Yan, Bin Bi, Jiabo Ye, Hehong Chen, Guohai Xu, Zheng Cao, et al. mplug: Effective and efficient vision-language learning by cross-modal skip-connections. *arXiv preprint arXiv:2205.12005*, 2022. 3
- [38] Junnan Li, Dongxu Li, Caiming Xiong, and Steven Hoi. Blip: Bootstrapping language-image pre-training for unified vision-language understanding and generation. In *International Conference on Machine Learning*, pages 12888–12900. PMLR, 2022.
- [39] Junnan Li, Dongxu Li, Silvio Savarese, and Steven Hoi. Blip-2: Bootstrapping language-image pre-training with frozen image encoders and large language models. *arXiv preprint arXiv:2301.12597*, 2023. 3
- [40] Raymond Li, Loubna Ben Allal, Yangtian Zi, Niklas Muenighoff, Denis Kocetkov, Chenghao Mou, Marc Marone, Christopher Akiki, Jia Li, Jenny Chim, et al. Starcoder: may the source be with you! *arXiv preprint arXiv:2305.06161*, 2023. 2, 3, 4, 5, 1
- [41] Tzu-Mao Li, Michal Lukáč, Michaël Gharbi, and Jonathan Ragan-Kelley. Differentiable vector graphics rasterization for editing and learning. *ACM Transactions on Graphics (TOG)*, 39(6):1–15, 2020. 1, 2, 5
- [42] Zicheng Liao, Hugues Hoppe, David Forsyth, and Yizhou Yu. A subdivision-based representation for vector image editing. *IEEE transactions on visualization and computer graphics*, 18(11):1858–1867, 2012. 2
- [43] Haotian Liu, Chunyuan Li, Qingyang Wu, and Yong Jae Lee. Visual instruction tuning. *arXiv preprint arXiv:2304.08485*, 2023. 3
- [44] Zhuang Liu, Hanzi Mao, Chao-Yuan Wu, Christoph Feichtenhofer, Trevor Darrell, and Saining Xie. A convnet for the 2020s. In *Proceedings of the IEEE/CVF conference on computer vision and pattern recognition*, pages 11976–11986, 2022. 3, 4, 8, 1
- [45] Raphael Gontijo Lopes, David Ha, Douglas Eck, and Jonathon Shlens. A learned representation for scalable vector graphics. In *Proceedings of the IEEE/CVF International Conference on Computer Vision*, pages 7930–7939, 2019. 2, 4, 5, 3
- [46] Ilya Loshchilov and Frank Hutter. Decoupled weight decay regularization. *arXiv preprint arXiv:1711.05101*, 2017. 6, 2
- [47] Xu Ma, Yuqian Zhou, Xingqian Xu, Bin Sun, Valerii Filev, Nikita Orlov, Yun Fu, and Humphrey Shi. Towards layer-wise image vectorization. In *Proceedings of the IEEE/CVF Conference on Computer Vision and Pattern Recognition*, pages 16314–16323, 2022. 1
- [48] Oscar Mañas, Pau Rodriguez, Saba Ahmadi, Aida Nematzadeh, Yash Goyal, and Aishwarya Agrawal. Mapl: Parameter-efficient adaptation of unimodal pre-trained models for vision-language few-shot prompting, 2023. 3
- [49] Kenton Murray and David Chiang. Correcting length bias in neural machine translation. *arXiv preprint arXiv:1808.10006*, 2018. 3
- [50] Erik Nijkamp, Bo Pang, Hiroaki Hayashi, Lifu Tu, Huan Wang, Yingbo Zhou, Silvio Savarese, and Caiming Xiong. Codegen: An open large language model for code with multi-turn program synthesis. *arXiv preprint arXiv:2203.13474*, 2022. 2, 3, 1
- [51] OpenAI. Gpt-4 technical report, 2023. 2, 3, 5
- [52] OpenAI. GPT-4V(ision) System Card. https://cdn.openai.com/papers/GPTV_System_Card.pdf, 2023. Accessed: 2023-11-05. 6, 2, 3
- [53] Adam Paszke, Sam Gross, Soumith Chintala, Gregory Chanan, Edward Yang, Zachary DeVito, Zeming Lin, Alban Desmaison, Luca Antiga, and Adam Lerer. Automatic differentiation in PyTorch. In *NeurIPS-W*, 2017. 6
- [54] Antoine Quint. Scalable vector graphics. *IEEE MultiMedia*, 10(3):99–102, 2003. 1
- [55] Alec Radford, Karthik Narasimhan, Tim Salimans, Ilya Sutskever, et al. Improving language understanding by generative pre-training. *openAI*, 2018. 3

- [56] Alec Radford, Jong Wook Kim, Chris Hallacy, Aditya Ramesh, Gabriel Goh, Sandhini Agarwal, Girish Sastry, Amanda Askell, Pamela Mishkin, Jack Clark, Gretchen Krueger, and Ilya Sutskever. Learning transferable visual models from natural language supervision. In *Proceedings of the 38th International Conference on Machine Learning*, pages 8748–8763. PMLR, 2021. [3](#)
- [57] Alec Radford, Jong Wook Kim, Chris Hallacy, Aditya Ramesh, Gabriel Goh, Sandhini Agarwal, Girish Sastry, Amanda Askell, Pamela Mishkin, Jack Clark, et al. Learning transferable visual models from natural language supervision. In *International conference on machine learning*, pages 8748–8763. PMLR, 2021. [2](#), [3](#), [4](#), [1](#)
- [58] Prajit Ramachandran, Barret Zoph, and Quoc V Le. Searching for activation functions. *arXiv preprint arXiv:1710.05941*, 2017. [4](#)
- [59] Aditya Ramesh, Mikhail Pavlov, Gabriel Goh, Scott Gray, Chelsea Voss, Alec Radford, Mark Chen, and Ilya Sutskever. Zero-shot text-to-image generation. In *International Conference on Machine Learning*, pages 8821–8831. PMLR, 2021. [3](#)
- [60] Aditya Ramesh, Prafulla Dhariwal, Alex Nichol, Casey Chu, and Mark Chen. Hierarchical text-conditional image generation with clip latents. *arXiv preprint arXiv:2204.06125*, 1(2):3, 2022. [3](#)
- [61] Pradyumna Reddy, Michael Gharbi, Michal Lukac, and Niloy J Mitra. Im2vec: Synthesizing vector graphics without vector supervision. *arXiv preprint arXiv:2102.02798*, 2021. [2](#), [4](#), [5](#), [6](#), [7](#)
- [62] Juan A Rodriguez, David Vazquez, Issam Laradji, Marco Pedersoli, and Pau Rodriguez. Figgen: Text to scientific figure generation. *arXiv preprint arXiv:2306.00800*, 2023. [8](#)
- [63] Juan A Rodriguez, David Vazquez, Issam Laradji, Marco Pedersoli, and Pau Rodriguez. Ocr-vqgan: Taming text-within-image generation. In *Proceedings of the IEEE/CVF Winter Conference on Applications of Computer Vision*, pages 3689–3698, 2023. [8](#)
- [64] Robin Rombach, Andreas Blattmann, Dominik Lorenz, Patrick Esser, and Björn Ommer. High-resolution image synthesis with latent diffusion models. In *Proceedings of the IEEE/CVF conference on computer vision and pattern recognition*, pages 10684–10695, 2022. [2](#), [3](#)
- [65] Baptiste Roziere, Jonas Gehring, Fabian Gloeckle, Sten Sootla, Itai Gat, Xiaoqing Ellen Tan, Yossi Adi, Jingyu Liu, Tal Remez, Jérémy Rapin, et al. Code llama: Open foundation models for code. *arXiv preprint arXiv:2308.12950*, 2023. [2](#), [8](#), [1](#)
- [66] Christoph Schuhmann, Romain Beaumont, Richard Vencu, Cade Gordon, Ross Wightman, Mehdi Cherti, Theo Coombes, Aarush Katta, Clayton Mullis, Mitchell Wortsman, et al. Laion-5b: An open large-scale dataset for training next generation image-text models. *Advances in Neural Information Processing Systems*, 35:25278–25294, 2022. [4](#), [1](#)
- [67] Louis Shao, Stephan Gouws, Denny Britz, Anna Goldie, Brian Strope, and Ray Kurzweil. Generating high-quality and informative conversation responses with sequence-to-sequence models. *arXiv preprint arXiv:1701.03185*, 2017. [3](#)
- [68] Noam Shazeer. Fast transformer decoding: One write-head is all you need. *arXiv preprint arXiv:1911.02150*, 2019. [4](#), [3](#)
- [69] Benjamin Spector and Chris Re. Accelerating llm inference with staged speculative decoding. *arXiv preprint arXiv:2308.04623*, 2023. [3](#)
- [70] Nitish Srivastava, Geoffrey Hinton, Alex Krizhevsky, Ilya Sutskever, and Ruslan Salakhutdinov. Dropout: a simple way to prevent neural networks from overfitting. *The journal of machine learning research*, 15(1):1929–1958, 2014. [1](#)
- [71] Nisan Stiennon, Long Ouyang, Jeffrey Wu, Daniel Ziegler, Ryan Lowe, Chelsea Voss, Alec Radford, Dario Amodei, and Paul F Christiano. Learning to summarize with human feedback. *Advances in Neural Information Processing Systems*, 33:3008–3021, 2020. [2](#)
- [72] Chengjun Tang, Kun Zhang, Chunfang Xing, Yong Ding, and Zengmin Xu. Perlin noise improve adversarial robustness. *arXiv preprint arXiv:2112.13408*, 2021. [2](#)
- [73] Hugo Touvron, Thibaut Lavril, Gautier Izacard, Xavier Martinet, Marie-Anne Lachaux, Timothée Lacroix, Baptiste Rozière, Naman Goyal, Eric Hambro, Faisal Azhar, et al. Llama: Open and efficient foundation language models. *arXiv preprint arXiv:2302.13971*, 2023. [3](#)
- [74] Hugo Touvron, Louis Martin, Kevin Stone, Peter Albert, Amjad Almahairi, Yasmine Babaei, Nikolay Bashlykov, Soumya Batra, Prajjwal Bhargava, Shruti Bhosale, et al. Llama 2: Open foundation and fine-tuned chat models. *arXiv preprint arXiv:2307.09288*, 2023. [2](#), [3](#)
- [75] Ashish Vaswani, Noam Shazeer, Niki Parmar, Jakob Uszkoreit, Llion Jones, Aidan N Gomez, Łukasz Kaiser, and Illia Polosukhin. Attention is all you need. *Advances in neural information processing systems*, 30, 2017. [2](#), [3](#)
- [76] Ashwin K Vijayakumar, Michael Cogswell, Ramprasath R Selvaraju, Qing Sun, Stefan Lee, David Crandall, and Dhruv Batra. Diverse beam search: Decoding diverse solutions from neural sequence models. *arXiv preprint arXiv:1610.02424*, 2016. [3](#)
- [77] Yael Vinker, Ehsan Pajouheshgar, Jessica Y Bo, Roman Christian Bachmann, Amit Haim Bermano, Daniel Cohen-Or, Amir Zamir, and Ariel Shamir. Clipasso: Semantically-aware object sketching. *ACM Transactions on Graphics (TOG)*, 41(4):1–11, 2022. [3](#)
- [78] Vision Cortex. VTracer. <https://www.visioncortex.org/vtracer-docs>, 2023. [2](#), [5](#), [6](#), [7](#)
- [79] Yizhi Wang and Zhouhui Lian. Deepvecfont: Synthesizing high-quality vector fonts via dual-modality learning. *ACM Transactions on Graphics (TOG)*, 40(6):1–15, 2021. [2](#)
- [80] Zhou Wang and Alan C Bovik. Mean squared error: Love it or leave it? a new look at signal fidelity measures. *IEEE signal processing magazine*, 26(1):98–117, 2009. [5](#)
- [81] Zhou Wang, Alan C Bovik, Hamid R Sheikh, and Eero P Simoncelli. Image quality assessment: from error visibility to structural similarity. *IEEE transactions on image processing*, 13(4):600–612, 2004. [5](#)

- [82] Thomas Wolf, Lysandre Debut, Victor Sanh, Julien Chaumond, Clement Delangue, Anthony Moi, Pierric Cistac, Tim Rault, Rémi Louf, Morgan Funtowicz, et al. Huggingface’s transformers: State-of-the-art natural language processing. *arXiv preprint arXiv:1910.03771*, 2019. 6
- [83] Ronghuan Wu, Wanchao Su, Kede Ma, and Jing Liao. Iconshop: Text-based vector icon synthesis with autoregressive transformers. *arXiv preprint arXiv:2304.14400*, 2023. 2, 3
- [84] Tong Wu, Liang Pan, Junzhe Zhang, Tai Wang, Ziwei Liu, and Dahua Lin. Density-aware chamfer distance as a comprehensive metric for point cloud completion. *arXiv preprint arXiv:2111.12702*, 2021. 5
- [85] Tian Xia, Binbin Liao, and Yizhou Yu. Patch-based image vectorization with automatic curvilinear feature alignment. *ACM Transactions on Graphics (TOG)*, 28(5):1–10, 2009. 2
- [86] Jiahui Yu, Yuanzhong Xu, Jing Yu Koh, Thang Luong, Gunjan Baid, Zirui Wang, Vijay Vasudevan, Alexander Ku, Yinfei Yang, Burcu Karagol Ayan, et al. Scaling autoregressive models for content-rich text-to-image generation. *arXiv preprint arXiv:2206.10789*, 2(3):5, 2022. 3
- [87] Richard Zhang, Phillip Isola, Alexei A Efros, Eli Shechtman, and Oliver Wang. The unreasonable effectiveness of deep features as a perceptual metric. In *Proceedings of the IEEE conference on computer vision and pattern recognition*, pages 586–595, 2018. 6

StarVector: Generating Scalable Vector Graphics Code from Images

Supplementary Material

In the following, we present a further description of the StarVector architecture, its training process, and how we generate SVG samples from images. We also provide more details about SVGBench with the proposed datasets as well as the different baselines within the evaluation setup. We also include additional results and discussions of our method for image-to-SVG generation.

7. Model Architecture

Code LLM. We consider several aspects in the choice of the code LLM to handle the SVG code generation. First, we require an LLM that is able to handle large token contexts during training, as SVG code samples are typically of long lengths (between 1000-4000 tokens, but growing arbitrarily for much more complex vector graphics). Second, we need fast decoding during the generation of these large contexts. Finally, we would benefit from models that have been extensively pre-trained on general coding tasks, to avoid early training costs. Some prior works offer open-source models that fit these requirements. We explored the open-source families of models CodeGen [50], and StarCoder [40]. We empirically found that StarCoder was the better option during our development stage as it allows a token context length of 8,192, a strong requirement of our complex SVG datasets (e.g., SVG-Emoji or SVG-Stack). We make use of the StarCoder1B model which fits well in our GPU training setup given that we include a large image encoder (i.e., CLIP) and need to manage gradients and activations for the image modality and long token sequences.

In the future, we will focus on scaling up the StarCoder model to 3, 7, and 16 billion parameters⁹, which we consider can bring benefits in learning to generate SVG of higher quality and complexity. Furthermore, the CodeLlama models [65] have shown remarkable coding performance and the possibility of scaling context length above our current 8,192 limit.

Image Encoder. Our image encoding pipeline consists of computing a set of feature representations from the images using a backbone image encoder and aligning them to the CodeLLM via the adapter module. State-of-the-art image encoders are typically focused on natural images. However, our data contains images of logotypes, icons, fonts, or emojis, which typically contain no background (which we set to white) and mostly constant colors. We explore several image encoders based on different paradigms. VQGAN [25] is based on learning to project images to discrete tokens. First,

we fine-tune an Imagenet [19]-pretrained VQGAN and fine-tune it with SVG-Stack on the proposed VQ-adversarial reconstruction task. We find that using the features before the quantization yields better results. ConvNext [44] is a convolutional backbone, which we extract features before pooling. We start from a LAION-2B [66]-pretrained checkpoint. Finally, ViT CLIP [57] is based on the Visual Transformer (ViT) [24] and is well prepared for autoregressive tasks. We extract all output representations. We use a LAION-2B pre-trained model. During the training of StarVector, all the parameters of the image encoders are updated. We find that the best choice is using CLIP. We consider that the gains in performance come from the fact that CLIP uses more visual tokens (257) than the other image encoders.

The adapter first projects the features from the original dimensionality D_v to a dimensionality $D_v \times 2$, followed by a Swish non-linear activation function, and a linear projection to the LLM dimensionality D_l . Finally, we apply a layer normalization [4]. We initialize the adapter parameters with Glorot [28]. Dropout [70] of 0.1 is applied at the beginning. These hyperparameters were found using a random search on SVG-Fonts.

From our results, we see that image resolution is important in order to capture fine-grained details like texts or high-frequency patterns. As seen in some examples (see Figure 19), diagrams and figures are part of the SVG-Stack dataset and present challenging horizontal or vertical aspect ratios. When images have these aspect ratios, we make the image fit in the 224×224 resolution, losing much detail, especially for the OCR capabilities of reading rendered texts and accurately displaying them.

Additional results comparing image encoders can be found in Figures 7 and 12. These results show the boost in precision obtained when using CLIP. VQGAN and ConvNext often fail at capturing the given shape of the image as well as the trajectory of the path. We note that ConvNext performs better than VQGAN. These differences are also due to the differences in the number of parameters. The CLIP ViT-L/14 model that we use consists of 290,581,504 parameters, VQGAN consists of 29,298,176, and ConvNext consists of 179,385,345 parameters.

Generating SVGs from natural images is out of the scope of this project. However, future work will focus on adapting our model to natural images, drawing from [47] and [11] to create a dataset of natural images and SVG pairs.

⁹<https://huggingface.co/blog/starcoder>

8. SVGBench

Here we extend our description of the datasets used for training and evaluating StarVector and other baselines. Earlier SVG datasets proposed in the literature (mainly datasets of emojis and fonts) were not easily accessible, due to broken URLs and no direct entry point. Therefore, we provide them as part of SVGBench for easy reproducibility. We introduce splits for train, validation, and testing. The train set is used to optimize the parameter weights of the network. The validation is used for tuning sampling hyperparameters, and the test is used for evaluation. Our model can handle up to 8k context tokens, therefore our datasets only consider examples with up to 8,192 tokens. See table 7 for a complete description of the datasets.

SVG Simplification. As mentioned before, DeepSVG requires a simplification of the SVG in its input. The simplification consists of eliminating complex primitives and using only vector paths. Also, color and shapes are abstracted to only use simple line strokes. We create simplified versions of the datasets Table 7 shows the complete datasets contained in SVG-Bench

9. Data augmentation for SVG

We introduce several augmentation operations to SVGs in order to apply slight changes that help our model learn to generate more precise results. For instance, being able to capture precise colors from the image and encode them in hexadecimal code to introduce it in the `fill` attribute of the SVG element. Applying rotations or adding noise to the control points of the curve helps the model learn to precisely capture the position of the edges or thickness of the stroke.

We perform random rotations in an angle range. We perform color changes by first parsing the color of the element using the `fill` attribute and adding small white Gaussian noise to the RGB values. We propose curve noise by injecting a small Perlin [72] noise into the control points in Bézier curves. We also experimented with adding Gaussian noise which resulted in much less natural results. We apply this noise by uniformly sampling a scalar from the interval between 0.01 and 0.05 and use it to scale the noise

We apply these augmentations directly on the SVG code, which involves parsing the XML code and accessing the attributes and arguments of the primitives defined. We use the libraries `BeautifulSoup`¹⁰ and `SvgPathTools`¹¹. Some primitives are simplified using our augmentations.

¹⁰<https://www.crummy.com/software/BeautifulSoup/bs4/doc/>

¹¹<https://github.com/mathandy/svgpathtools>

10. Training

For training the StarVector model we define the task of image-to-SVG conversion as learning to map a sequence of image token embeddings (or visual tokens) to a sequence of SVG code token embeddings. It can be seen as a sequence-to-sequence problem modeling the translation between the image and the SVG code domains.

The goal of StarVector is to estimate the conditional probability $p(y_1, \dots, y_m | x_1, \dots, x_n)$, where x_1, \dots, x_n is the input sequence of image tokens and y_1, \dots, y_m is the output sequence of SVG tokens. n corresponds to the length of the image token sequence, which is fixed and defined by the image encoder (see Section 3) and m is the variable size of the SVG code tokens. Denoting $X = (x_1, \dots, x_n)$ we compute this conditional probability as

$$p(y_1, \dots, y_m | X) = \prod_{t=1}^m p(y_t | X, y_1, \dots, y_{t-1}), \quad (2)$$

where the distribution $p(y_t | X, y_1, \dots, y_{t-1})$ is represented using a softmax over the LLM vocabulary of tokens.

As described in Section 7 we make use of a CLIP image encoder and a non-linear adapter to obtain a sequence of image token embeddings (we refer to them as visual tokens)

We find that this general task makes the model learn to draw vectors that look like the image. Notably, this task can be learned without supervision in the image domain, only relying on a categorical cross-entropy loss on the LLM vocabulary introduced by the next-token prediction task.

We use a batch size of 2. Images are processed with a resolution of 224x224, as defined by the pre-trained CLIP image encoder, and process a maximum of 8192 tokens, considering the 257 tokens for representing the images (visual tokens) and the rest for the SVG tokens. We use gradient batch accumulation of 8, and we train on a data parallel setup with 4 A100 80GB GPUs, having an effective batch size of 64. The learning rate is set to 5×10^{-4} for training, using AdamW optimizer [46] for approximately 5 days of training on SVG-Stack dataset.

11. Baselines

We reproduce all previous approaches in SVGBench, as the available results come from an unclear version of the fonts, emojis, and icons datasets. Namely, we run DeepSVG [13] and Im2Vec [61] using the official implementations. We used the hyperparameters proposed by the authors and utilized pre-/post-processing code as needed. We use the recent GPT4 Vision [52] model capable of processing images as input and producing SVG code in the output. We also run VTracer on our data, which is a rule-based method (i.e., not learning from data).

Dataset	Train	Val	Test	Source	Avg. Token Length	SVG Primitives
SVG-Fonts	1,831,857	91,593	4,821	Glypazzn [45]	2,121 ± 1,868	Vector path
SVG-Fonts _{sim}	1,436,391	71,789	3,745		1,722 ± 723	Vector path
SVG-Emojis	8,708	667	668	OpenMoji, NotoEmoji, TweMoji	2,551 ± 1,805	All
SVG-Emojis _{sim}	580	57	96		2,448 ± 1,026	Vector Path
SVG-Icons	80,442	6,256	2,449	DeepSVG [13]	2,449 ± 1,543	Vector path
SVG-Icons _{sim}	80,435	2,836	1,277		2,005 ± 824	Vector path
SVG-Stack	2,169,710	108,456	5,709	TheStack [36]	1,822 ± 1,808	All
SVG-Stack _{sim}	601,762	30,061	1,585		2,042 ± 918	Vector path

Table 7. Complete datasets on SVG-Bench. The subscript *sim* stands for the simplified version of the dataset.

Im2Vec. We scaled down all the images to 128×128 resolution to be compatible with the Im2Vec model. We use a learning rate of 5×10^{-4} and a batch size of 8. We implement a custom post-processing operation for converting the vector parameters obtained during Im2Vec inference to obtain compilable SVG code.

DeepSVG. This model can only handle simplified SVGs composed of simple line strokes and splines (see examples in Figure 3). Further, it can only process SVGs with 8 groups (i.e., groups of shapes, or parent nodes) and vector paths of at most 30 commands. To reproduce the DeepSVG baseline, we use the original hyperparameters, including a learning rate of $1e-3$ and a number of epochs to be 50. We use a batch size of 200, except for the smaller emoji dataset, where we experiment with a batch size of 50.

VTracer. We use the Python library¹² for experiments which is a wrapper over the Rust implementation. Similar to Im2Vec, we scale down all the images to 128×128 resolution. We use all the default values for the rule-based engine which generates a multi-colored SVG.

GPT-4 Vision (preview). GPT-4 Vision [52] offers multimodal capabilities for handling image and text data for tasks like image captioning, or text-image interleaved conversation. Here we show how one can use prompt engineering [9, 10, 52] to condition the model to generate executable SVG code that represents the given image. Figure 9 displays the prompt that we use for this endeavor. We use the OpenAI library¹³ to perform experiments with GPT-4-Vision. Notably, the currently available model `gpt-4-vision-preview` has a limit of 100 queries per day, which only allows us to report results on 100 examples per dataset (see Table 3).

SVG generation prompt

You are a helpful assistant. Your task is to help researchers in writing SVG code to reconstruct the provided image as similar as possible. You should also provide a caption of the image. You are devoted to solve the task of image to svg conversion for a robust system, hence you always have to respond with the best svg you can. Please feel free to use multiple paths to generate a compilable SVG code in max 8000 tokens. You should respond with the svg that best reconstructs the input image in triple quotes. \n\n Caption: \n\n SVG:

Figure 9. Prompt used for SVG Generation from GPT-4-V.

12. Sampling from StarVector

Here we describe how we sample SVG code from our model. As a decoder-only LLM [40], StarVector first computes the key-value (KV) cache using the visual tokens from the image and produces the initial set of output logits. This stage is often quick because the model can process the entire visual token sequence simultaneously [69]. The selected token from the output logits is then input back into the model, which in turn generates logits for the subsequent token. This process is iteratively repeated until the model produces the desired quantity of tokens. Our approach uses architectural improvements for fast decoding such as FlashAttention [18] and Multi-Query Attention [68].

To select the correct sampling temperature we perform a grid on SVG-Emoji and SVG-Icons validation sets. Figure 10 shows that the choice of temperature does not strongly impact the results. However, a 1-point increase in performance is observed on CD for SVG-Emoji using temperatures close to 1.0. We also present an ablation study on popular decoding techniques [31, 49, 67, 76]. Specifically, we experiment with greedy decoding, beam search, and nucleus sampling with $\text{top-}p$. Results are shown in Table 8. The use of nucleus sampling with $\text{top-}p=0.9$ and temperature $T=0.5$ (no beam search) shows to be the best option. The use of beam search improves the greedy decoding baseline, but it does not work well when combined with nucleus sampling, increasing the inference time. In sum, we recom-

¹²https://github.com/etjones/vtracer_py

¹³<https://platform.openai.com/docs/libraries>

Sampling technique	SVG-Fonts				SVG-Emojis				SVG-Icons				SVG-Stack			
	MSE ↓	CD ↓	LPIPS ↓	SSIM ↑	MSE ↓	CD ↓	LPIPS ↓	SSIM ↑	MSE ↓	CD ↓	LPIPS ↓	SSIM ↑	MSE ↓	CD ↓	LPIPS ↓	SSIM ↑
Greedy	0.013	2.255	0.019	0.969	0.071	2.133	0.251	0.731	0.028	1.156	0.059	0.912	0.067	13.350	0.157	0.797
+ Beam Search (B=5)	0.012	2.250	0.018	0.970	0.070	2.130	0.250	0.732	0.027	1.150	0.058	0.913	0.066	13.340	0.156	0.798
Nucleus Sampling (T=0.5)	0.008	2.098	0.013	0.976	0.051	2.194	0.202	0.778	0.022	0.483	0.043	0.923	0.072	6.153	0.153	0.785
Nucleus Sampling (T=1.0)	0.009	2.214	0.015	0.975	0.067	2.083	0.244	0.742	0.025	0.714	0.053	0.917	0.069	7.100	0.161	0.786
+ Beam-Search (B=5)	0.027	2.792	0.034	0.948	0.068	3.449	0.244	0.742	0.027	1.028	0.065	0.913	0.089	11.278	0.195	0.766
+ Beam-Search (B=10)	0.031	3.093	0.040	0.943	0.072	3.537	0.251	0.742	0.028	1.173	0.071	0.910	0.079	10.052	0.175	0.762

Table 8. **Ablation study on sampling strategies.** We experiment using greedy decoding and add beam search with B=5. We test nucleus sampling [31] using top p=0.9, with temperatures T=0.5 and T=1.0. The two final rows describe the use of beam search with nucleus sampling at T=1.0. See huggingface.co/blog/how-to-generate for reference on these sampling techniques.

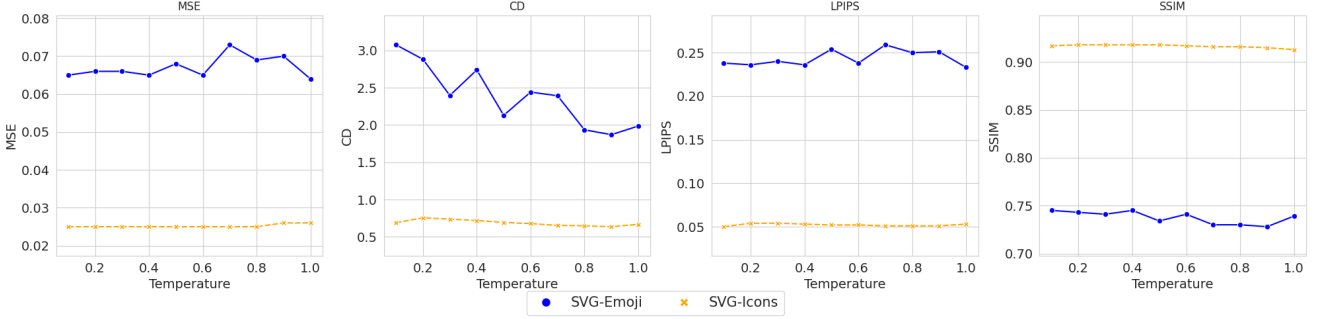


Figure 10. **Ablation study on sampling temperature.** We test our methods’ performance impact when changing the sampling temperature. Results are computed for SVG-Emoji and SVG-Icons validation sets.

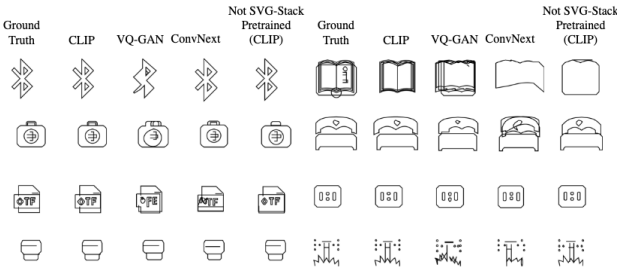


Figure 11. Ablation study on SVG-Icons full test set

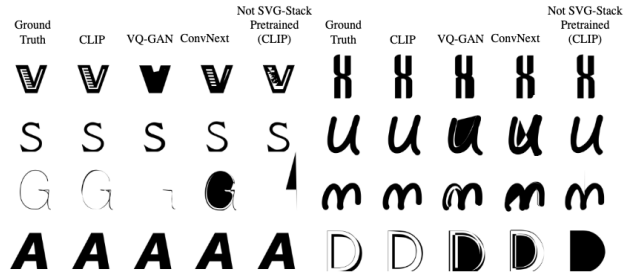


Figure 12. Ablation study on SVG-Fonts full test set

mend nucleus sampling [31] with top p=0.9 and temperature between 0.5 and 0.9 for the best performance.

Assuring SVG Compilation. A common problem when generating SVGs with our approach is that sometimes the maximum token length of the generated SVG might not be sufficient for completing the code, and compilation errors may appear. We find that only training with SVG code that fits in the context length allows for obtaining around 85% of compilation success. The remaining incomplete samples are post-processed with `cairosvg` in order to obtain a complete and compilable SVG. Nevertheless, some parts of the image are lost in some cases. In future work, we will explore techniques to address this issue, as some other works have introduced [6].

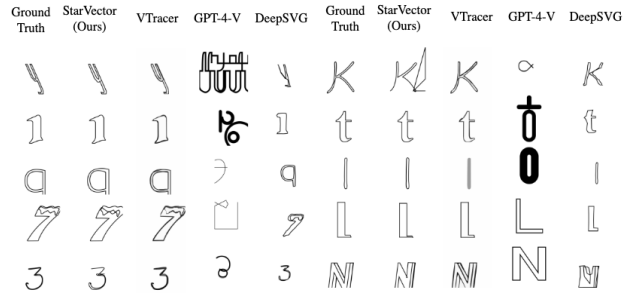


Figure 13. Baseline predictions on SVG-Fonts simplified test set

13. Additional results

We facilitate some additional experiments and ablations performed with StarVector.

13.1. Additional SVG samples generated

Figures [14 - 19] show substantial qualitative samples generated by StarVector on all the proposed datasets. All results are computed in the test sets. We can observe the weaknesses and strengths of our model. Simplified datasets (Figures 15 and 17) are near-perfectly converted to SVG, however, sometimes the model runs out of SVG code tokens and the image is incomplete. Sometimes the model generates unnecessary loops, making the ability to stop earlier. Results on SVG-Emoji 16 show impressive performance in estimating the shape’s color and semantics. However, it lacks fine-grained and accurate positioning of objects. These problems result from the lack of sufficient emoji samples. We consider that this problem can be alleviated by scaling on model parameters, data, and computing resources. Results on SVG-Fonts 14 are notably good, as StarVector is able to represent detailed high-frequency patterns (see "A" example from row 7, column 1). The good performance comes from the large data regime on this dataset.

13.2. Comparison to Baselines

Here we discuss the results on each baseline individually, comparing it to our proposed approach.

DeepSVG DeepSVG [13] is an elegant approach to learning a latent variable model for SVG, and it proves effective at learning the task for the simplified datasets (see Figure 3 and 13). Results show that it is able to represent accurately corners and edges in all datasets. Nevertheless, the limitation in the complexity of SVGs restricts it from being a suitable solution in real applications.

Im2Vec We find it difficult to fit the Im2Vec [61] model to our data. When reproducing the proposed training setup in our datasets, the model does not progress in training. Their proposed training procedure does not require having SVG ground truth and uses only pixel-based reconstruction loss. It requires a differentiable rasterizer like DiffVG [41] to find the optimal SVG parameters. This framework is very appealing, as it aims to be used in images with no SVG supervision. However, it requires hundreds of epochs with a reduced dataset, to overfit the model to those examples, only working on modeling training examples, as seen in [61]. This training objective makes it difficult to find good solutions, especially on large SVG datasets like the ones in SVGBench, which Im2Vec is not able to handle.

GPT-4 Vision GPT-4 Vision (GPT-4V) does a great job at capturing the semantics of the image. It also does very well at capturing the colors of the input image and representing them in the SVG code (see Figure 20). However, it is not able to compete in terms of reconstruction fidelity. GPT-4V

was not trained for the task of reconstruction, hence these result is expected.

VTracer VTracer outperforms our model in multiple settings. It works especially well when the image can be easily segmented into clear regions based on color or texture. However, it tends to fail on images that contain high-frequency patterns, like vector images with white backgrounds and small polygon shapes close to each other with different colors. For instance, examples from rows 2 and 3 in Figure 6 in VTracer show how it is not able to precisely vectorize small details of shapes, letters, or color change. When the image contains several lines that are close together in fine-grained patterns, the details tend to be lost (see the example in Figure 3 row 3 column 3). VTracer is also limited by the primitives it is able to generate, restricted only to vector paths. Some capabilities like optical character recognition and the conversion of text rendered using the `<text>` tag can not be attained by rule-based models.

Therefore, seeing the complete set of results, we consider that the StarVector approach is the only deep learning method on image-to-SVG that can obtain comparable results to VTracer. Further, StarVector opens novel research avenues for generating vector graphics, that could support useful problems such as text-to-SVG or improved editing and understanding.

Ground Truth Generated Ground Truth Generated Ground Truth Generated Ground Truth Generated Ground Truth Generated Ground Truth Generated

5	5	a	a	i	i	b	b	A	A	I	I
B	B			4	4	U	U	N	N	Z	Z
i	i	x	x	P	P	/	/	ſ	ſ	o	o
V	V	r	r	n	n	Y	Y	†	†	A	A
k	k	W	W	W	W	O	O	F	F	Q	Q
8	8	1	1	T	T	\	\	U	U	W	W
A	A	X	X	Z	Z	t	t	N	N	ÿ	ÿ
8	8	E	E	o	o	U	U	ſ	ſ	i	i
Y	Y	n	n	A	A	Z	Z	U	U	T	T
w	w	T	T	k	k	o	o	J	J	F	F

Figure 14. Generated samples from SVG-Fonts test.



Figure 15. Generated samples from SVG-Fonts simplified test.



Figure 16. Generated samples from SVG-Emoji test.



Figure 17. Generated samples from SVG-Icons test.



Figure 18. Generated samples from SVG-Stack test (i).



Figure 19. Generated samples from SVG-Stack test (ii).

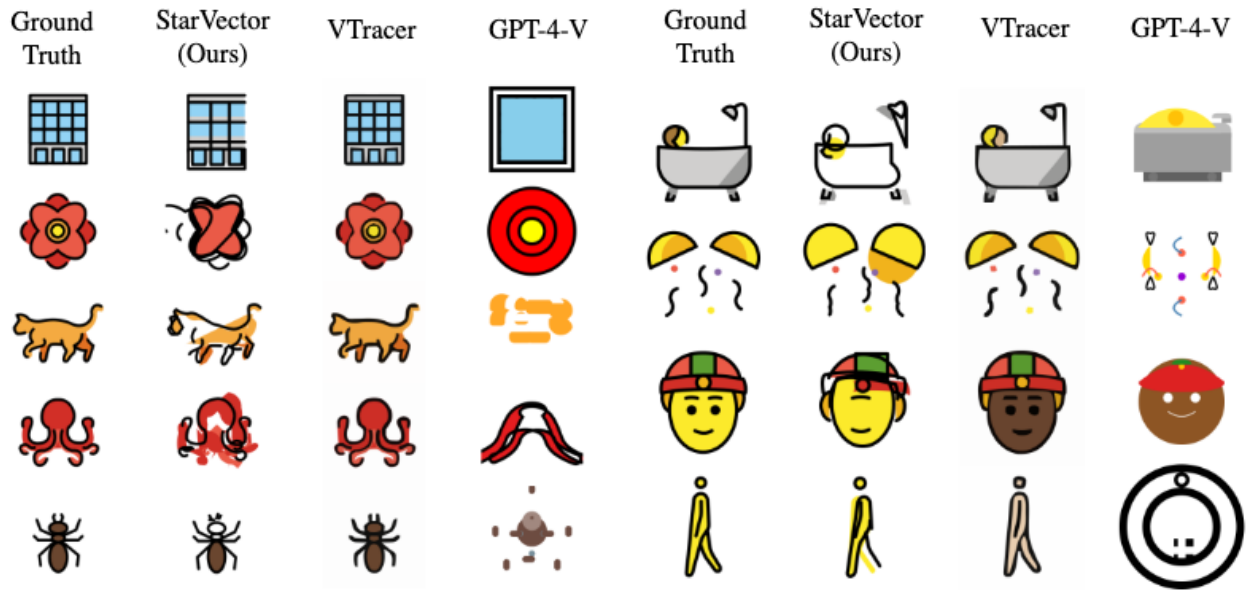


Figure 20. Baseline comparison of generated examples on SVG-Emoji test set

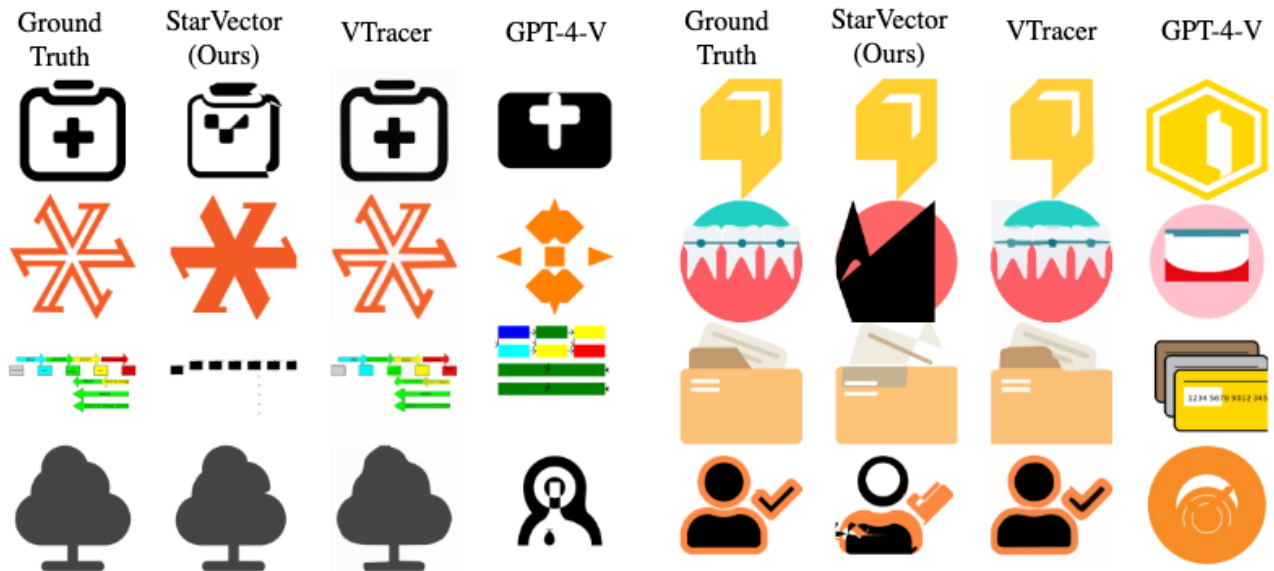


Figure 21. Baseline comparison of generated examples on SVG-Stack test set